Decoherence of a quantum memory coupled to a collective spin bath

Richard Walters,[1,*] Stephen R. Clark,[2,1] and Dieter Jaksch[1,2]

[1] *Clarendon Laboratory, University of Oxford, Oxford, OX1 3PU, UK*

[2] *Centre for Quantum Technologies, National University of Singapore, 3 Science Drive 2, Singapore 117543*

(Dated: May 27, 2010)

We study the quantum dynamics of a single qubit coupled to a bath of interacting spins as a model for decoherence in solid state quantum memories. The spin bath is described by the Lipkin-Meshkov-Glick model and the bath spins are subjected to a transverse magnetic field. We investigate the qubit interacting via either an Ising- or an XY-type coupling term to subsets of bath spins of differing size. The large degree of symmetry of the bath allows us to find parameter regimes where the initial qubit state is revived at well defined times after the qubit preparation. These times may become independent of the bath size for large baths and thus enable faithful qubit storage even in the presence of strong coupling to a bath. We analyze a large range of parameters and identify those which are best suited for quantum memories. In general we find that a small number of links between qubit and bath spins leads to less decoherence and that systems with Ising coupling between qubit and bath spins are preferable.

PACS numbers: 03.67.-a,03.65.Yz

Keywords: Quantum memory, spin bath, decoherence, non-Markovian dynamics, Loschmidt echo, entanglement breaking

I. INTRODUCTION

The transfer and storage of quantum information between different physical systems is of crucial importance to quantum communication and distributed quantum computing [1]. Experimentally quantum communication is one of the most advanced areas of quantum technology with promising commercial applications being a realistic possibility in the near future [2]. However, for its full potential to be realized over relevant distances, limitations caused by noisy transmission lines, e.g. the exponential scaling of photon losses in an optical fiber with its length, need to be overcome.

Several promising proposals to solve this problem exist. The most well studied is the use of quantum repeaters which segment the transmission line into shorter pieces [3, 4]. By applying sophisticated entanglement purification schemes and entanglement swapping at these repeater units, high-fidelity entangled pairs can be established over much larger distances than direct transmission could feasibly permit. A recent alternative method has been proposed that is based on the idea of entanglement percolation in a quantum network. Given nodes that are initially connected by partially entangled pure states [5] or mixed states [6], schemes based on classical bond percolation have been shown to enable the creation of maximally entangled singlet states between arbitrary points in the network with a probability independent of the distance between them [7]. Both quantum repeater and percolation schemes require that quantum information is stored locally at the repeaters or nodes of the network and crucially their operation degrades in the presence of decoherence in these memories.

In this work we investigate the quantum dynamics of a single qubit quantum memory coupled to an environment of interacting spin-1/2 particles [8]. Such a model of decoherence has relevance for solid-state quantum memories involving the nuclear spin [9, 10], electron spin in a semiconducting quantum dot [11] and nitrogen vacancy centers in diamond [12]. Previous studies examining the decoherence induced by spin baths have mostly considered the so-called 'central spin model' in which the qubit is coupled isotropically to all spins in the bath. Early work has analyzed the decoherence due to independent bath spins [13–16], whilst most studies since have investigated 1D models with nearest-neighbor couplings [17–22]. The effect of an infinite-range interaction amongst bath spins has also been studied within the central spin model [23–26]. However, as pointed out by Rossini *et al.* in Ref. [27], the assumption of a central spin may not be valid for many physical systems. Thus, in their work [27] the authors depart from the central spin model and consider just a few links between the qubit and a 1D spin chain. Here we consider the spin bath as being described by the Lipkin-Meshkov-Glick (LMG) model (see Eq. 3), which possesses infinite-range interactions, and similarly go beyond the central spin model by examining the decoherence of a single qubit as its exposure to the spin bath is varied from coupling to just one bath spin through to interacting with all bath spins.

The LMG spin bath represents an ideal benchmark for investigating the effects of the varying qubit interactions with a non-trivial spin bath. Firstly, it possesses permutational symmetry, which can be exploited to exactly solve its dynamics numerically for very large number of spins ($\sim$ 100-1000). This in itself is a rare property for many-body quantum systems. The large degree of symmetry in the bath also allows us to identify parameter regimes where highly non-Markovian [15] coherence prop-

* r.walters1@physics.ox.ac.uk

erties are displayed within the quantum memory. We quantify this by its rephasing time and periodic entanglement breaking, which are found to be independent of the bath size. Secondly, the LMG model has also attracted much attention [28–32] for exhibiting either first- or second-order equilibrium quantum phase transitions dependent on the type of intra-bath coupling. As is now well known the entanglement properties of the ground state are strongly affected at criticality [33–36] and this in turn can have a profound effect on the induced decoherence of a coupled qubit [17]. We explore the effects of criticality and in a similar fashion to H. T. Quan *et al.* in Ref. [17] our findings point to a possible use of a coupled quantum memory as an apparatus for the dynamical measurement of a QPT through its coherence properties.

The structure of this paper is as follows. In Sec. II we introduce the model and the bath Hamiltonian, and describe the ground state properties of the bath under various parameter regimes. We also introduce the dephasing Ising interaction and dissipative XY interaction terms and discuss the measures used to quantify decoherence in our system. The results are presented in Sec. III and IV for dephasing and dissipative interactions respectively, with conclusions drawn in Sec. V.

II. THE MODEL

The model under consideration is that of a single spin-1/2 (qubit) Q interacting with a spin bath R. The purpose of the investigation is two-fold: the primary focus is to study how the interaction with the bath affects the evolution of Q, however in doing so we also use Q as a probe to study the bath dynamics across criticality. The Hamiltonian of the global system, depicted schematically in Fig. 1 is of the standard form

$$H_T = H_Q + H_R + H_I \ , \tag{1}$$

where H_Q and H_R are the free Hamiltonians of the qubit and the bath respectively, and H_I is the interaction term. For the qubit we assume

$$H_Q = -\omega \varsigma^z \ , \tag{2}$$

where ς^z is the Pauli z-operator and ω is the energy difference between the ground and excited states; we work in units with $\hbar = 1$. In the following subsections, we will introduce the bath Hamiltonian $H_R = H_{LMG}$ and the two different interaction terms under consideration. Throughout this work, the subsystems Q and R will be initiated at time $t = 0$ in a product state, with the bath in its ground state.

A. The Lipkin-Meshkov-Glick bath

The bath is described by the Lipkin-Meshkov-Glick model, which was originally proposed in nuclear physics

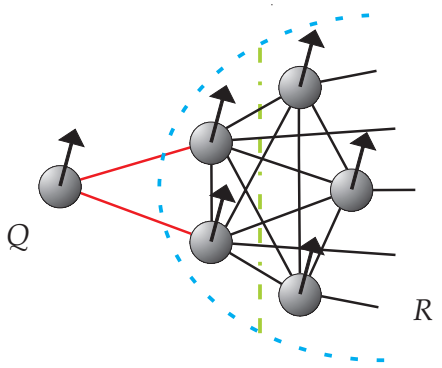

FIG. 1. (Color on line) A schematic of the model under investigation. A single spin-1/2 is coupled via k links (red lines) to a completely connected spin bath R. Note that the lengths of the lines do not correspond to the strength of the interactions. The green dash-dotted line indicates a particular bath partition.

to describe shape phase transitions in nuclei [37]. We note that it has since found relevance in describing the Josephson effect in two-mode Bose-Einstein condensates [38] and a dissipative implementation of it has also recently been proposed in optical cavity QED [39]. The model involves a system of N spins-1/2 mutually interacting in the x-y plane and embedded in a transverse magnetic field. The Hamiltonian is given by

$$\begin{aligned} H_{LMG} &= -\frac{\lambda}{N}\sum_{i<j}^{N}(\sigma_i^x\sigma_j^x + \gamma\sigma_i^y\sigma_j^y) - h\sum_{i=1}^{N}\sigma_i^z \\ &= -\frac{2\lambda}{N}(S_x^2 + \gamma S_y^2) - 2hS_z + \frac{\lambda}{2}(1+\gamma) \ , \end{aligned} \tag{3}$$

where $S_\alpha = \sum_{i=1}^{N}\sigma_i^\alpha/2$ is the collective spin operator for the direction $\alpha = x, y, z$; and the σ^α are the Pauli operators for spins in the bath. The quantities λ, h, and γ characterize the interaction strength between bath spins, the magnetic field strength, and the anisotropy in the x-y plane, respectively. The above Hamiltonian describes an infinite-ranged XY model, with the prefactor $1/N$ on the first term necessary to ensure a finite free energy per spin in the thermodynamical limit. The cases $\gamma = 1$ and $\gamma = 0$ correspond to infinite-ranged XX and transverse Ising models respectively. In the following, we consider only ferromagnetic interactions $\lambda > 0$ within the bath for anisotropy values $0 \leq \gamma \leq 1$.

The mutual coupling of all spins described by H_{LMG} results in the energy eigenstates of the free bath being invariant under particle exchange. Furthermore, H_{LMG} commutes with the total spin operator $\mathbf{S}^2 = S_x^2 + S_y^2 + S_z^2$, and so the energy eigenstates are divided into symmetric subspaces $\mathbb{S}_S$ defined by the spin quantum number S of $\mathbf{S}^2$ and each of dimensionality $2S + 1$. This symmetry vastly reduces the complexity of studies of the ground state (GS) of the bath. For ferromagnetic intra-bath couplings the GS lies in the maximal spin subspace $\mathbb{S}_{N/2}$, and so its calculation is an eigenvalue problem scaling as just

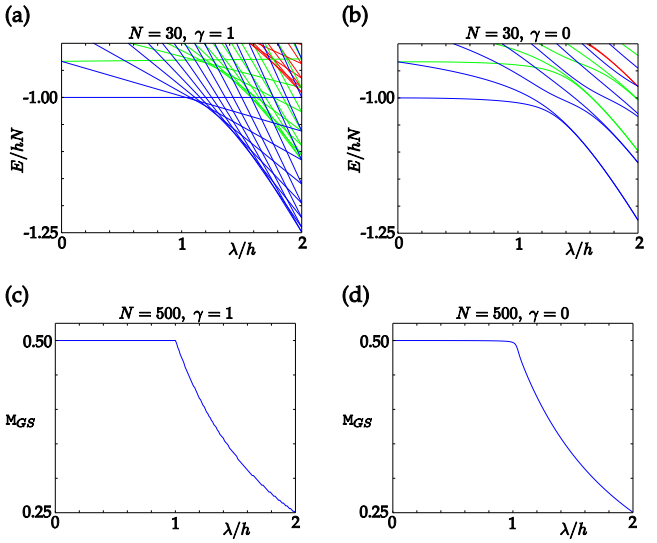

FIG. 2. (Color on line) Upper: the energy spectrum for isotropic (a) and anisotropic (b) ferromagnetically coupled baths of $N = 30$ spins. Blue lines indicate levels in the subspace $\mathbb{S}_{N/2}$, green lines the subspace $\mathbb{S}_{(N/2)-1}$, and red lines the subspace $\mathbb{S}_{(N/2)-2}$. Lower: GS magnetization (per spin) in the z-direction for isotropic (c) and anisotropic (d) ferromagnetically coupled baths of $N = 500$ spins.

$N + 1$.

For isotropic intra-bath coupling ($\gamma = 1$) H_{LMG} also commutes with S_z and is thus diagonal in the symmetric eigenbasis spanned by Dicke states $|S, M\rangle$ [40] (M is the quantum number for S_z). Dicke states are degenerate except for those belonging to the maximal spin subspace $\mathbb{S}_{N/2}$. For an ensemble of N spins, Dicke states in the subspace $\mathbb{S}_{N/2}$ are entangled states except for the two spin-polarized states $|N/2, N/2\rangle$ and $|N/2, -N/2\rangle$.

1. *Ground state properties*

The ground state of the ferromagnetic bath lies in the maximal spin subspace $\mathbb{S}_{N/2}$ for all γ and $\lambda > 0$. A mean-field approach [41, 42] predicts a second-order quantum phase transition in the thermodynamical limit at the critical point $\lambda = h$ for all $\gamma \geq 0$.

For a finite, isotropic bath there is a crossing of the lowest energy levels at $\lambda_c = hN/(N-1)$. This is shown in Fig. 2(a), where we have plotted the energies $E = \langle H_{LMG}\rangle$ of the lowest levels for $\gamma = 1$. The GS is the separable, spin-polarized state $|N/2, N/2\rangle$ for $0 \leq \lambda \leq \lambda_c$ (normal phase), and an entangled state $|N/2, \lfloor hN/2\lambda \rceil\rangle$ for $\lambda > \lambda_c$ (broken phase), where the function $\lfloor x \rceil$ rounds x to the nearest integer. For both phases the GS is non-degenerate for any bath size. Note that the critical point depends on h, thus the bath can be directed to either phase by setting the magnetic field strength correspondingly greater or less than the intra-bath coupling strength.

The GS of an anisotropic bath is a superposition over all Dicke states in the maximal spin subspace $\mathbb{S}_{N/2}$, but tends to the spin-polarized state $|N/2, N/2\rangle$ in the limit $\lambda \to 0$. The GS is non-degenerate for the normal phase, but becomes doubly degenerate in the thermodynamical limit for the broken phase. This is demonstrated in Fig. 2(b), which shows that the energies of the lowest levels are almost identical for an anisotropic bath of just $N = 30$ spins. In the thermodynamical limit, the GS magnetization (per spin) in the z-direction is given by

$$\mathtt{M}_{GS} = \frac{1}{N}\langle S_z\rangle = \begin{cases} 1/2 & \text{for } 0 \leq \lambda \leq h \\ h/2\lambda & \text{for } \lambda \geq h \end{cases}, \qquad (4)$$

for all γ. See Figs. 2(c) and 2(d) for the magnetization of a large but finite bath with $\gamma = 1$ and $\gamma = 0$ respectively.

2. *Analytical calculations with a partitioned LMG bath*

The high symmetry of the LMG bath allows us to easily compute exact solutions of the system dynamics for a large number of spins, since the GS can be expressed in a reduced subspace $\mathbb{S}_S$ scaling at most as $N + 1$. However, this representation of the GS is limited in that we can only consider operators that are symmetric across the entire bath ensemble. Fortunately, the LMG model provides some flexibility since we can make partitions of the bath, as shown in Fig. 1, without significantly increasing the scaling with system size, and thus can also consider non-symmetric operators. As an example, consider an operator that acts on, and is symmetric across, a total of k bath spins. We make a bipartite split of the bath into subsystems A and B with k and $N - k$ spins respectively, and transform the original Dicke states as

$$|(s_A, s_B)S, M\rangle = \sum_{m_A, m_B} |s_A, m_A\rangle \otimes |s_B, m_B\rangle \times \langle s_A, m_A| \otimes \langle s_B, m_B|S, M\rangle \ , \qquad (5)$$

where $|s_A, m_A\rangle$ and $|s_B, m_B\rangle$ are Dicke states for subsystems A and B; $s_A \leq k/2$; and $s_B \leq (N-k)/2$. We denote the tensor product space by $\mathbb{S}^k_{s_A} \otimes \mathbb{S}^{N-k}_{s_B}$, where the superscripts indicate the corresponding number of spins. On the LHS of Eq. (5) we specify s_A and s_B because, in general, there are a range of allowed values these quantum numbers can take when coupling to form $|S, M\rangle$. However, for the case where S is maximal, which is our only concern, we have $s_A = k/2$, $s_B = (N-k)/2$ and $s_A + s_B = S$, reducing the Clebsch-Gordan coefficients in Eq. (5) from the general form in Ref. [43] to

$$\langle k/2, m_A| \otimes \langle (N-k)/2, m_B|N/2, M\rangle = \delta_{m_A+m_B,M}\sqrt{\frac{F_{m_A+k/2}(k)F_{m_B+(N-k)/2}(N-k)}{F_{M+N/2}(N)}}\ , \tag{6}$$

where $F_b(a) = a!/[b!(a-b)!]$ are binomial coefficients. From Eqs. (5) and (6) we can construct a transformation operator that maps the subspace $\mathbb{S}_{N/2}$ to the tensor product space $\mathbb{S}^k_{k/2} \otimes \mathbb{S}^{N-k}_{(N-k)/2}$, given by

$$T_{N/2\to k/2,(N-k)/2} = \sum_{M=-N/2}^{N/2}\sum_{m_A=-k/2}^{k/2}\sum_{m_B=-(N-k)/2}^{(N-k)/2}\delta_{m_A+m_B,M}\sqrt{\frac{F_{m_A+k/2}(k)F_{m_B+(N-k)/2}(N-k)}{F_{M+N/2}(N)}} \times |k/2, m_A\rangle \otimes |(N-k)/2, m_B\rangle\langle N/2, M|\ . \tag{7}$$

We apply this transformation operator to the representations in $\mathbb{S}_{N/2}$ of both the GS and H_{LMG}, allowing us to consider operators that are symmetric across just k spins without needing to revert to the full Hilbert space $\mathbb{C}_2^{\otimes N}$.

B. Ising interaction

The first interaction term we consider is of the Ising type

$$H_I = \frac{\epsilon}{\sqrt{k}}\varsigma^z \otimes \sum_{i=1}^{k}\sigma_i^z\ , \tag{8}$$

where ϵ is the interaction strength. This commutes with the free qubit Hamiltonian (i.e. $[H_I, H_Q] = 0$) and thus there will be no energy exchange between the qubit and the bath; the evolution will affect the off-diagonal terms of the state of Q only. The term above describes a situation involving a total of k out of N bath spins interacting with the qubit. By using the transformation operator in Eq. (7) we can vary the value of k to study any scenario from a single coupled bath spin ($k = 1$) to a completely coupled bath (i.e. the central spin model, $k = N$), allowing us to evaluate how the evolution of the qubit changes as it is exposed to varying numbers of bath spins. We have introduced the factor $1/\sqrt{k}$ so as not to artificially increase the interaction strength as we increase the number of links, effectively normalizing the interaction term.

C. LMG interaction

With the second interaction we allow energy exchange between the qubit and the bath and thus introduce dissipation into the subsystem Q. A natural way of doing this is to consider the qubit interacting with the bath spins in the same way the bath spins do with each other, i.e.

$$H_I = \frac{\epsilon}{\sqrt{k}}\sum_{i=1}^{k}(\varsigma^x \otimes \sigma_i^x + \gamma\varsigma^y \otimes \sigma_i^y)\ . \tag{9}$$

The anisotropy parameter γ used here is the same as that in the LMG Hamiltonian in Eq. (3). Once again, we vary k from 1 to N in order to consider different levels of exposure of the qubit to the bath.

D. Characterizing decoherence

The main aim of this work is to characterize how the coupling to an LMG spin bath affects the decoherent evolution of the qubit Q. In the following subsections we introduce two measures that allow us to do this; namely, the average purity, and whether the induced decoherence is 'entanglement breaking'. Their calculation requires the use of an ancilla qubit and exploits the Jamiolkowski isomorphism [44], which is detailed in appendix A. Importantly, all the information pertaining to the decoherent evolution of the single qubit is mapped via the Jamiolkowski isomorphism to a two-qubit state ρ^Λ for Q and the ancilla. From ρ^Λ we can ascertain if and when the evolution is entanglement breaking, and also deduce the Kraus operators for the evolution to obtain the average purity.

1. *Average purity*

We use the purity of the reduced quantum state $\rho(t)$ of the qubit, defined as $P[\rho] \equiv \mathrm{Tr}(\rho^2)$, as a measure of its decoherent evolution in the presence of the bath. The qubit state at time t will be pure iff $P(t) = 1$, and mixed for $P(t) < 1$. We initialize the qubit in a pure state at $t = 0$ so that any mixing of the state, i.e. decoherence, can be observed in its subsequent evolution described by the unital map $\varepsilon\{\rho(0)\}$. In general, the purity depends on the exact details of the state at $t = 0$ and thus we average over all possible initial pure states $|\psi\rangle$ to obtain the average purity. This can be achieved once the Kraus operators A_i for the evolution are known via [45]

$$\begin{aligned}\overline{P} &= \overline{\mathrm{Tr}[\varepsilon\{|\psi\rangle\langle\psi|\}^2]}^{\psi} \\ &= \frac{1}{d(d+1)}\left(\sum_{ij=1}^{d^2}\left|\mathrm{Tr}[A_i^\dagger A_j]\right|^2 + d\right)\ ,\end{aligned} \tag{10}$$

where $d = 2$ is the dimension of the quantum subsystem.

2. Entanglement breaking

A useful property to determine environmentally induced decoherence is whether it destroys any entanglement the primary subsystem Q has with an external subsystem. The superoperator Λ (see appendix A) describing the effect of the interaction is 'entanglement breaking' [46] if, when acting on a subsystem b of dimension d_b, the final state $\rho_{ab}^{fin} = \mathbb{1} \otimes \Lambda_a(\rho_{ab}^{ini})$ is separable for every (possible entangled) initial state ρ_{ab}^{ini} of the composite system of b and an external subsystem a of dimension d_a (not necessarily a copy of b). Importantly, when the state ρ^{Λ} obtained as described in appendix A is separable, the superoperator Λ will be entanglement breaking since this implies the corresponding quantum operation ε has a Kraus representation composed entirely of projectors. Separability can be determined, using the positive partial transposition (PPT) criterion [47, 48], by computing the minimum eigenvalue $\mu(t)$ of the matrix $(\rho^{\Lambda})^{T_a}$. The induced decoherence will be entanglement breaking iff $\mu(t) \geq 0$.

III. RESULTS: ISING INTERACTION

In this section we present results for the single spin decoherence induced by the Ising interaction with the LMG bath spins. Before doing so, it is useful to discuss exactly how decoherence arises in this system.

Consider the qubit initially prepared in a generic superposition of its ground and excited states, such that the global state at time $t = 0$ is

$$|\Psi(0)\rangle = \big(a_0|0\rangle + a_1|1\rangle\big) \otimes |GS\rangle \ , \tag{11}$$

where the coefficients a_0 and a_1 satisfy $|a_0|^2 + |a_1|^2 = 1$. The subsequent evolution under H_T for times $t > 0$ is described by

$$\begin{aligned} |\Psi(t)\rangle = a_0 e^{-i\omega t}|0\rangle \otimes e^{-iH_+ t}|GS\rangle \\ + a_1 e^{i\omega t}|1\rangle \otimes e^{-iH_- t}|GS\rangle \ , \end{aligned} \tag{12}$$

where $S_z^k = \sum_{i=1}^k \sigma_i^z/2$, and $H_\pm = H_R \pm 2\epsilon S_z^k/\sqrt{k}$ are perturbed bath Hamiltonians. In general, the bath evolves to different states dependent on whether the qubit was initially in the state $|0\rangle$ or $|1\rangle$, and therefore Eq. (12) is an entangled state of the two subsystems. After tracing out the bath we obtain the reduced density matrix for the qubit (in the eigenbasis $\{|0\rangle, |1\rangle\}$)

$$\rho(t) = \mathrm{Tr}_R\{|\Psi(t)\rangle\langle\Psi(t)|\} = \begin{pmatrix} |a_0|^2 & \rho_{12}(t) \\ \rho_{12}^*(t) & |a_1|^2 \end{pmatrix}, \tag{13}$$

where

$$\rho_{12}(t) = a_0 a_1^* e^{-2i\omega t} D^*(t) \ . \tag{14}$$

The relative populations of the ground and excited states of the qubit are conserved, but dephasing noise is introduced through the decoherence factor

$$D(t) = \langle GS|e^{iH_+ t} e^{-iH_- t}|GS\rangle \ . \tag{15}$$

Note that the induced decoherence is independent of ω. The purity of the state in Eq. (13) is

$$P[\rho(t)] = 1 - 2|a_0|^2|a_1|^2\left[1 - L(t)\right] \ , \tag{16}$$

where $L(t) \equiv |D(t)|^2$ is a real quantity taking the form of a Loschmidt Echo (LE) [49] for the bath. Unlike the purity, $L(t)$ is independent of the initial state of the qubit, aside from the fact that it is undefined for $a_0 = 0, 1$. Thus, the average purity is trivially related to the LE via $\overline{P(t)} = [2 + L(t)]/3$.

By the term Loschmidt Echo we mean that $L(t)$ quantifies the distance between the two bath states that have evolved from the GS under the two perturbed bath Hamiltonians $H_\pm$. When the distance between these states is small, the entanglement between the qubit and the bath is low and the average purity is close to one. Conversely, when the LE is zero the two time-evolved bath states are orthogonal and the qubit is maximally entangled with the bath. In such cases, the qubit undergoes total dephasing to a completely mixed state and the average purity takes its minimum value of 2/3. Also, this type of dephasing noise is entanglement breaking iff $L(t) = 0$ [46].

A useful quantity to consider that will give insight into how the decoherence varies with link number k is the Fourier Transform of the decoherence factor in Eq. (15), given by

$$\chi(E) = \sum_{i,j} \langle GS|\phi_i^+\rangle\langle\phi_i^+|\phi_j^-\rangle\langle\phi_j^-|GS\rangle\delta(E - E_j^- + E_i^+) \ , \tag{17}$$

where $|\phi_i^\pm\rangle$ are eigenvectors of the perturbed bath Hamiltonians $H_\pm$, and $E_i^\pm$ their eigenenergies. Contributions to $\chi(E)$ occur at energy differences $E_j^- - E_i^+$ corresponding to eigenstates $|\phi_j^-\rangle$ and $|\phi_i^+\rangle$ that simulaneously connect to (i.e. are not distant from) each other and the bath GS.

A. Single link, $k = 1$

The simplest case to consider first is that of a single link between the qubit and the bath. In particular, for an isotropic bath ($\gamma = 1$) the GS in the normal phase ($\lambda < h$) is the spin-polarized state $|N/2, N, 2\rangle$, which is an eigenstate of both perturbed bath Hamiltonians $H_\pm$. The bath remains in the GS for the entirety of the evolution and simply induces an additional z-rotation on the initial qubit state through an angle $2\epsilon t$, thus there is zero dephasing.

In the broken phase ($\lambda > h$) we observe a loss of qubit coherence and find that the average purity has an oscillatory behavior with time, as shown in Fig. 3(a). For an isotropic bath, we show in appendix B that the GS in the broken phase decomposes into two terms when we move to the bipartite subspace $\mathbb{S}_{1/2}^1 \otimes \mathbb{S}_{(N-1)/2}^{N-1}$. The evolution of the bath under $H_\pm$ is further confined to a subspace

comprising only the two states of the decomposition, allowing us to describe the bath propagators $e^{-iH_{\pm}t}$ by 2 x 2 matrices (see Eqs. (B9) and (B10)). The resulting expression for the purity is too complicated to be given explicitly, however, we can extract the salient behavior from the form of the two propagators. The off-diagonal matrix elements of $e^{-iH_{-}t}$ vary sinusoidally such that it periodically becomes equal to the identity matrix with a frequency $\eta_{-} = 2\sqrt{\lambda^2 + \epsilon(\epsilon + 2h)}$ that is independent of bath size N. Similarly, $e^{-iH_{-}t}$ varies periodically with a frequency $\eta_{+} = 2\sqrt{\lambda^2 + \epsilon(\epsilon - 2h)}$. When both propagators are the identity at the same time, the LE becomes unity and there is a revival of full qubit coherence. This 'coherence time' τ_c must simultaneously satisfy $\eta_{-}\tau_c = 2l_{-}\pi$ and $\eta_{+}\tau_c = 2l_{+}\pi$, where l_{-} and l_{+} are integers. In general, we observe fast oscillations of the average purity determined by the higher frequency η_{-}, which are contained within an envelope function that is periodic with a frequency η_{+}. High average purities of $\overline{P(t,\lambda)} > 0.98$ are obtained at times $t = l\tau_r$ (l an integer), where $\tau_r = \pi/\eta_{+}$ is the approximate 'rephasing time' corresponding to the first maximum of the envelope function. This is plotted in Fig. 3(b) for various values of the interaction strength ϵ. In the limit $\epsilon \ll h$, the frequencies $\eta_{\pm}$ are approximately equal and a full revival of qubit coherence occurs at a time $\tau_c \sim \tau_r = \pi/\lambda$. For $\epsilon = h$ the rephasing time is asymptotic at $\lambda = h$, and thus its sensitivity to small changes in the magnetic field allows for an observation of criticality. However, criticality should be avoided if one wishes to use the system for storage of the qubit state so that rephasing can occur on short-time scales.

The behavior described above for the coupling to an isotropic bath is independent of bath size N. Thus, the revivals of qubit coherence are not a finite size effect and occur in the thermodynamical limit. This independence with N arises because the bath Hamiltonian takes a particularly simple form for $\gamma = 1$ that is diagonal in the eigenbasis spanned by Dicke states $|S, M\rangle$, ultimately restricting the evolution to just a two-dimensional subspace. As a result, the decoherence factor has a maximum of four Fourier components, as shown in Fig. 3(c); there is only a single component in the normal phase where no dephasing occurs. Interestingly, when we consider anisotropic baths such that the evolution utilizes the entire $\mathbb{S}^1_{1/2} \otimes \mathbb{S}^{N-1}_{(N-1)/2}$ subspace, we find there are still only $n = 4$ significant Fourier components to the decoherence factor. Significant Fourier components are those of greatest amplitude that reproduce 98% of the signal. Also, we observe a rapid convergence of the average purity to the isotropic bath result with increasing bath size. In Fig. 3(d) we have plotted the average purity across criticality at time $t = 5/h$ for various bath anisotropies and a bath of $N = 100$ spins. Away from criticality, the average purity for all bath anisotropies is within 5% of the isotropic result for a bath of this size. Close to criticality the convergence is slower, and we observe oscillations in the average purity in the normal phase that disappear in the thermodynamical limit.

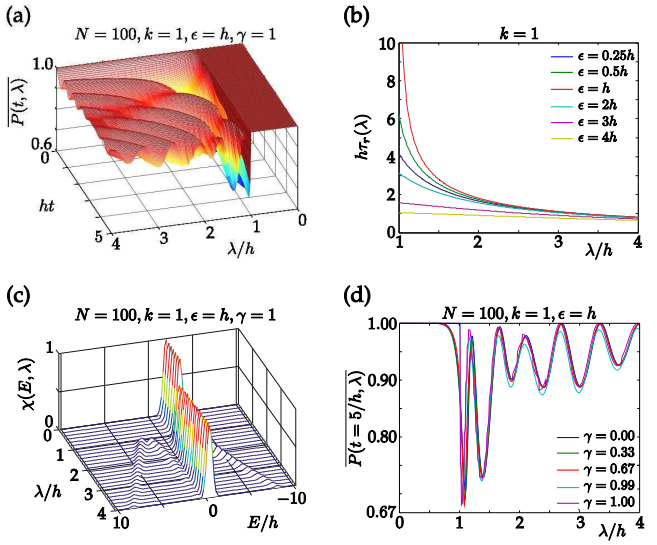

FIG. 3. Ising interaction, single link ($k = 1$): (a) the average purity plotted against λ and t. (b) The approximate rephasing time τ_r plotted against λ for various values of ϵ. (c) The Fourier Transform of the decoherence factor as a function of energy and λ. We have used Gaussian envelopes at each Fourier component for ease of viewing. (d) The average purity plotted against λ, at $t = 5/h$, for various values of γ.

B. Completely connected, $k = N$

We now consider the opposite extreme where the qubit is coupled to all spins in the bath, i.e. the central spin model. For an isotropic bath the average purity is trivially equal to one for all λ; the interaction term commutes with the bath Hamiltonian and thus the qubit and the bath cannot become entangled. The qubit experiences a z-rotation through an angle $\epsilon N t$ in addition to that of its free evolution [50].

Figure 4(a) shows a color map of the average purity against λ and t for an anisotropic bath ($\gamma = 0$) with $\epsilon = 0.25h$. At this low interaction strength the average purity is qualitatively similar to the single link scenario; there is almost zero dephasing in the normal phase, whilst oscillations occur within an envelope function in the broken phase. The rephasing time τ_r is asymptotic at criticality but contrary to the single link scenario we find it is independent of ϵ. As would be expected for this description the Fourier Transform of the decoherence factor for low interaction strengths is qualitatively similar to that shown in Fig. 3(c); there is one Fourier component with a large amplitude accompanied by a few ($n < 15$) of smaller amplitude.

As the interaction strength is increased above $\epsilon = h$ the behavior becomes markedly different. The maxima in the average purity are suppressed and, as shown in Fig. 4(b) for $\epsilon = 5h$, high average purities are no longer achieved on

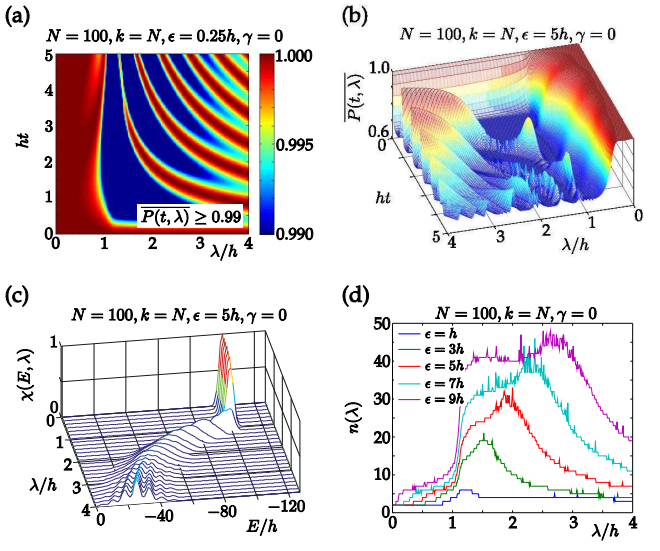

FIG. 4. Ising interaction, completely connected ($k = N$): (a) a colour map of the average purity plotted against λ and t for $\epsilon = 0.25h$. The map has a threshold at $\overline{P} = 0.99$ to improve clarity. (b) The average purity plotted against λ and t for $\epsilon = 5h$. (c) The Fourier transform of the decoherence factor as a function of energy and λ for $\epsilon = 5h$; again, we have used Gaussian envelopes at each Fourier component. (d) The number of Fourier components n of greatest amplitude that reproduce 98% of the signal, plotted against λ, and for various values of ϵ.

short-time scales, except in the limit $\lambda \to 0$. In addition, away from the maxima the LE is close to zero indicating that the evolution is almost entanglement breaking. The Fourier Transform of the decoherence factor for $\epsilon = 5h$, shown in Fig. 4(c), contains a large number n of significant components but no single one of high amplitude, resulting in the suppression of the maxima. In Fig. 4(d) we have plotted n across criticality for various values of ϵ. The number of significant Fourier components increases rapidly as we move from the normal to the broken phase, and contrary to the single link scenario increases at all intra-bath coupling strengths with ϵ.

Interestingly, for any ϵ the energy spread and number of components rapidly converge to finite values with increasing bath size. Thus, although at high interaction strengths there is a decay of qubit coherence on short-time scales, full revivals will eventually occur for any ϵ even in the thermodynamical limit, with the coherence time τ_c independent of N for large baths, $N \gtrsim 100$. Finally, we note that the behavior described in this subsection is only qualitatively the same for different bath anisotropies and does not tend to the isotropic behavior in the limit $\gamma \to 1$.

C. Multiple links

In the previous two subsections we have seen approximate rephasing occurs on short-time scales for any interaction strength when the qubit is connected via a single link to the bath, whilst for a completely connected qubit rephasing is suppressed at high interaction strengths. We now examine how this transition occurs as we gradually increase the number of links from the scenario $k = 1$ to $k = N$. We consider an intra-bath coupling strength of $\lambda = 3h$ such that we are away from criticality and rephasing is possible on short-time scales for any link number.

In Figs. 5(a) and 5(c) we have plotted the maximum value of the average purity for rephasing within a time $t \leq 10/h$, as a function of the interaction strength ϵ, and for a range of link numbers k. The bath size is $N = 50$. High average purities of $\overline{P} > 0.98$ are achieved for any link number below $\epsilon \sim 4h$, whilst above this interaction strength a high average purity is only guaranteed for $k < 3$. At higher link numbers we observe the suppression of maxima up to $\epsilon \sim 10h$ as discussed in Sec. III B for a completely connected bath. Interestingly, above $\epsilon = 10h$ the maxima in the average purity increase back towards one, with the rate of increase slowest for link numbers $k \sim$ 30-40. This behavior is prevalent when we consider the number of significant Fourier components n as a function of link number and interaction strength, shown in Fig. 4(b). For a few link numbers, we have $n < 10$ for all ϵ allowing approximate rephasing to occur. For higher link numbers, the number of components increase with ϵ up to a maximum value at $\epsilon \sim 10h$, before decreasing once more at higher interaction strengths. The number of components also has a maximum at $k \sim 35$ and therefore decreases with large k, but albeit is still relatively large for a completely connected qubit.

The restriction of the number of significant Fourier components can be explained by considering the form of the perturbed bath Hamiltonians $H_\pm = H_R \pm 2\epsilon S_z^k/\sqrt{k}$. At low interaction strengths $\epsilon < h$, the perturbing terms are small and the eigenstates of the two Hamiltonians are similar. There are approximately $(k+1)(N-k+1)$ terms $\langle \phi_i^+ | \phi_j^- \rangle$ that are non-zero, but only a few of these will connect to the GS and thus $\chi(E)$ will have only a few components. As the interaction strength is increased above $\epsilon = h$, the two sets of eigenstates differ meaning that there are now $(k+1)^2(N-k+1)^2$ non-zero-terms $\langle \phi_i^+ | \phi_j^- \rangle$, each of which will be of smaller magnitude. There is a larger set of pairs of eigenstates to connect to the GS leading to many more components. When the interaction strength is increased further such that the second terms dominate in $H_\pm$, the eigenstates again become similar and the number of components asymptotically decreases to one in the limit $\epsilon \to \infty$. The maximum in the number of components with link number arises because the subspace $\mathbb{S}^k_{k/2} \otimes \mathbb{S}^{N-k}_{(N-k)/2}$ is largest for $k = N/2$, however the maximum is skewed towards $k = N$ so that a completely connected qubit still has a relatively large number of components compared to the case $k = 1$.

Finally, we note that although the maxima in the average purity depend on link number, the minima do not, as shown in figure 5(d). The minima decrease towards, but do not reach, the minimum value of 2/3 (corresponding

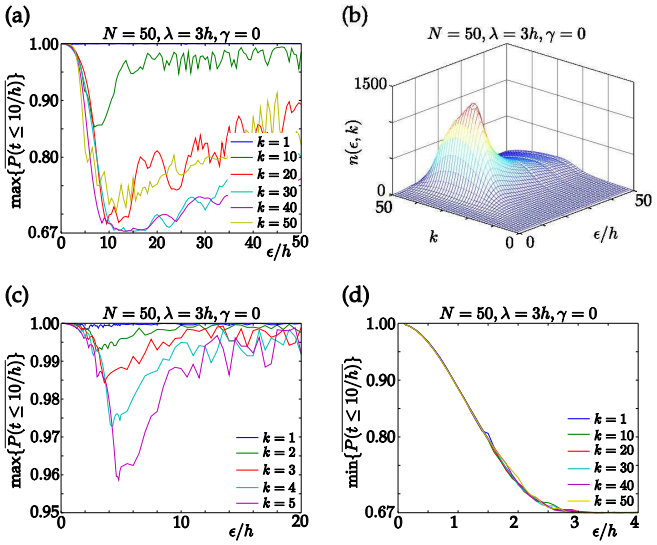

FIG. 5. Ising interaction: (a) the maximum value of the Loschmidt Echo at $\lambda = 3$ for rephasing within a time $t \leq 10/h$, as a function of ϵ, and for a range of k. (b) The number of Fourier components n of greatest amplitude that reproduce 98% of the signal as a function of ϵ and k. (c) same as (a) but for only a few links. (d) The minimum value of the Loschmidt Echo within $t \leq 10/h$ at $\lambda = 3$, plotted against ϵ.

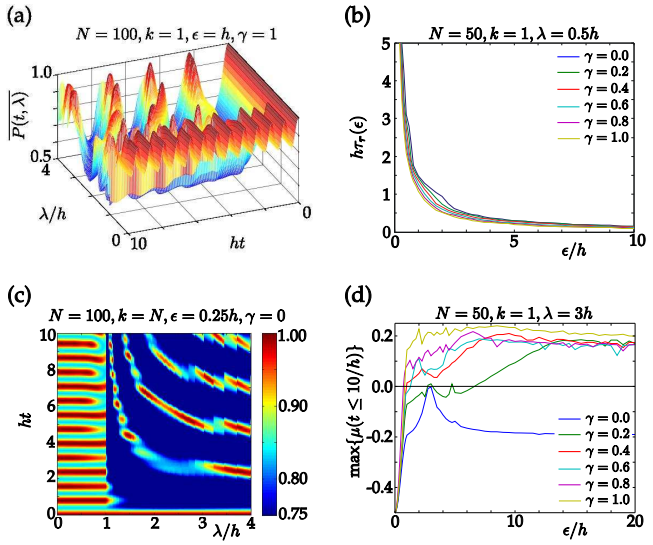

FIG. 6. LMG interaction, single link ($k = 1$): (a) the average purity plotted against λ and t for $\gamma = 1$. (b) The rephasing time τ_r for the bath in the normal phase ($\lambda = 0.5$), as a function of ϵ and for various values of γ. (c) A color map of the average purity plotted against λ and t for $\epsilon = h$. The map has a threshold at $\overline{P} = 0.75$ to improve clarity. (d) The maximum value of $\mu(t)$ within $t \leq 10/h$ at $\lambda = 3h$, as a function of ϵ and for various values of γ. Values above zero indicate that the evolution is entanglement breaking.

to an LE of zero) with increasing interaction strength and so the interaction is never formally entanglement breaking.

IV. RESULTS: LMG INTERACTION

We now present the results for the qubit interacting with the bath spins via the dissipative LMG interaction. Contrary to the Ising interaction, the relative populations of the ground and excited states of the qubit can vary in time in addition to the coherence. This means the average purity can take a minimum value of 1/2, but more significantly it is now dependent on the energy difference ω between the two levels of the qubit. In the following, we consider the scenario [51] in which the qubit is subject to an identical external field as the bath spins, thereby setting $\omega = h$. In tests where ω was varied decoherence was suppressed in all cases as ω was increased, thus the scenario considered is in the worst-case regime.

One important consideration for the LMG interaction, in contrast to the Ising interaction, is that the induced decoherence is non-trivially dependent on the initial qubit state. This means that the purity for a given initial state can have significantly different behavior to the average purity, and indeed can be unity when the average purity is not. It is interesting in the following results that we observe the average purity oscillating away from and back to unity, indiciating universal rephasing at certain times for any given initial qubit state. The evolution is also entanglement breaking for certain periods, which is shown in the following results using the quantity $\mu(t)$ discussed in Sec. II D 2.

A. Single link, $k = 1$

In Fig. 6(a) we have plotted the average purity for the qubit connected via a single link to an isotropic bath ($\gamma = 1$) with an interaction strength $\epsilon = h$. For the LMG interaction the average purity is not equal to unity in the normal phase for an isotropic bath, but instead we observe approximate revivals with a rephasing time τ_r that is independent of intra-bath coupling strength λ. The rephasing time increases rapidly with interaction strength and is almost independent of bath anisotropy, as shown in Fig. 6(b). The interaction is never entanglement breaking for any γ or ϵ in this phase.

As for the Ising interaction, we observe approximate revivals in the broken phase for all γ and ϵ. The rephasing time τ_r behaves in a similar fashion to the Ising case with a single link: it is almost independent of γ; increases with interaction strength up to $\epsilon = h$ where it is asymptotic at criticality (see Fig. 6(c)); and decreases at higher interaction strengths. In Fig. 6(d) we have plotted the maximum value of $\mu(t)$ within a time $t \leq 10/h$ for various bath anisotropies. We observe that the induced decoherence is periodically entanglement breaking in time for $\gamma > 0.1$ and interaction strengths $\epsilon > 8h$.

For the LMG interaction we again find that the average

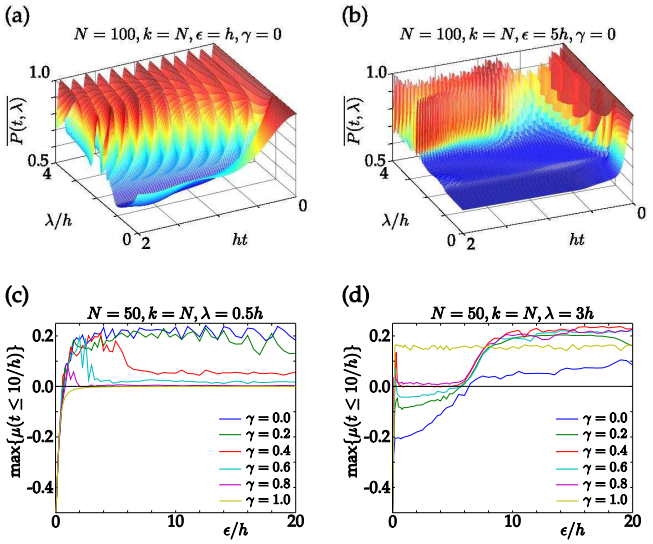

FIG. 7. LMG interaction, completely connected ($k = N$): (a) and (b), the average purity plotted against λ and t for $\gamma = 0$ and interaction strengths $\epsilon = h$ and $\epsilon = 5h$ respectively. (c) and (d), the maximum value of $\mu(t)$ within $t \le 10/h$ at $\lambda = 0.5h$ and $\lambda = 3h$ respectively, as a function of ϵ and for various values of γ. Values above zero indicate that the evolution is entanglement breaking.

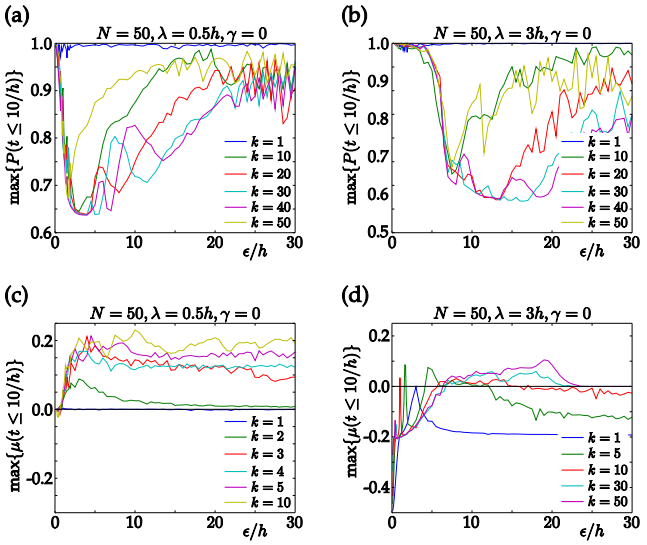

FIG. 8. LMG interaction: (a) and (b), the maximum value of the purity at $\lambda = 0.5h$ and $\lambda = 3h$ respectively, for rephasing within a time $t \le 10/h$, as a function of interaction strength ϵ and for various values of k. (c) and (d), the maximum value of $\mu(t)$ within $t \le 10/h$ at $\lambda = 0.5h$ and $\lambda = 3h$ respectively, as a function of ϵ and for various values of k. Values above zero indicate that the evolution is entanglement breaking.

purity is independent of bath size for large N. Thus, not only would we observe revivals in the thermodynamical limit, but interestingly they will occur after periods when the induced decoherence is entanglement breaking.

B. Completely connected, $k = N$

Figures 7(a) and 7(b) show the average purity, as a function of intra-bath coupling strength and time, for a completely connected qubit with $\gamma = 0$ and interaction strengths $\epsilon = h$ and $\epsilon = 5h$ respectively. For this bath anistropy there is a decay of the average purity in the normal phase even at low interaction strengths. Note that the decay also occurs at $\lambda = 0$ for which the bath spins do not interact with each other, and extends across criticality into the broken phase at high interaction strengths $\epsilon \gtrsim h$. Rephasing only occurs on short-time scales in the limit $\gamma \to 1$, with the rephasing time τ_r independent of bath size for large baths, $N \gtrsim 100$. The interaction is now entanglement breaking in this phase on short-time scales except in the limit $\gamma \to 1$, as shown in Fig. 7(c).

Approximate revivals occur in the broken phase away from criticality with a frequency much greater than that of the corresponding single link scenarios. Contrary to the Ising case, the rephasing time τ_r increases with interaction strength and converges less rapidly towards a finite value with increasing bath size. Therefore, the rephasing time can only be considered independent of bath size for very large baths, $N \gtrsim 1000$. Figure 7(d) shows that the induced decoherence is now periodically entanglement breaking on short-time scales for all γ above $\epsilon \sim 6h$ in this phase. However, at higher interaction strengths this is no longer the case; for $\gamma = 0$ the decoherence is not entanglement breaking for $\epsilon > 23h$ (see Fig. 8(d)).

C. Multiple links

As was the case for the Ising interaction, for the dissipative LMG interaction we observe a change in the qubit's behavior as we move from a single link to fully connected to the bath. In this subsection we discuss how this transition occurs as we vary the link number k for $\gamma = 0$. For this bath anisotropy approximate rephasing occurs on short-time scales in both phases for a single link, but is suppressed in the normal phase for $k = N$. Also, the decoherence is never entanglement breaking for $k = 1$ with $\gamma = 0$, but is at high interaction strengths for $k = N$. We consider intra-bath coupling strengths away from criticality of $\lambda = 0.5h$ for the normal phase and $\lambda = 3h$ for the broken phase.

Figures 8(a) and 8(b) show the maximum value of the average purity for rephasing within $t \le 10/h$ with a bath of $N = 50$ spins. Both figures are qualitatively similar to Fig. 5(a) for the Ising interaction; approximate rephasing occurs for a single link at any interaction strength, whilst the maxima in the average purity are suppressed at high interaction strengths for greater link numbers. In the broken phase, high average purities of $\overline{P} > 0.98$ are achieved for any link number below $\epsilon \sim 4h$, whilst in the normal phase this isn't the case and there is an

immediate decay of the average purity above $\epsilon = 0$ for $k \neq 1$. As for the Ising interaction, the suppression of maxima is reduced as the interaction strength is further increased, with the rate of increase slowest for link numbers $k \sim 30$-40. This suggests that our analysis discussed in Sec. III C, where the induced decoherence was limited by the size of the subspace required to describe the partitioned bath states, has a broader applicability than the Ising interaction alone. Rephasing depends on the number of significant Fourier components for, in this case, the average purity. This quantity is reduced in the limits $\epsilon \ll h$ and $\epsilon \gg h$ for which the interaction term is a small perturbation on the bath Hamiltonian and vice versa respectively.

In Figs. 8(c) and 8(d) we have plotted the maximum value of $\mu(t)$ within $t \leq 10/h$ for the normal and broken phases respectively. In the normal phase entanglement breaking occurs for $k \neq 1$ at interaction strengths $\epsilon > 0.8h$, whilst in the broken phase the induced decoherence is entanglement breaking for $k \neq 1$ within the range $h < \epsilon < 23h$. It is only the case of coupling via a single link that the qubit is immune to entanglement breaking within the period $t \leq 10/h$.

V. CONCLUSIONS

To summarize, we have investigated the quantum evolution of a single qubit coupled to a Lipkin-Meshkov-Glick bath as a model for decoherence in solid state quantum memories. The bath, which exhibited a second-order quantum phase transition, was highly symmetric and allowed for exact calculations of the system dynamics for large system sizes, $N \sim 100$ spins. Further, partitioning of the bath was possible without significantly increasing the computational complexity, which allowed us to determine the effect of increasing exposure of the qubit to the bath spins. Decoherence of the qubit was quantified using the average purity and determining if and when the evolution destroys any entanglement the qubit may have with an external subsystem.

For the qubit interacting via an Ising interaction with just a few bath spins, we observed zero dephasing in the normal phase and almost complete revivals of qubit coherence in the broken phase. The rephasing time, which was sensitive to criticality in the bath, was independent of bath size for large baths and thus faithful qubit storage would be possible in the thermodynamical limit. In general, as the number of links was increased the revivals in the purity were suppressed, which was discussed in terms of the number of components in the Fourier Transform of the decoherence factor. Decoherence was suppressed by the restrictive size of the subspace required to describe the partitioned bath states, which was smallest for just a few links. Further, it is likely that revivals were observed in certain scenarios, even in the thermodynamical limit, because the symmetry of the bath constrained the dynamics to a subspace whose dimension grows only linearly with system size. Such revivals could possibly occur in other systems possessing exchange symmetry that are not as easily amenable to analysis as the LMG model. However, they may be difficult to observe experimentally due to a potential lack of the required bath symmetry in real samples.

In contrast to the Ising interaction, for the dissipative XY-type (LMG) interaction between the qubit and the bath, decoherence was dependent on the energy difference between the two levels of the qubit and additionally was observed in both bath phases. Revivals were found to occur for certain parameter regimes and just a few links between the qubit and the bath. These were once again suppressed as the link number was increased, broadening our analytical discussion for the case of the Ising interaction in terms of the restrictive size of the bath's Hilbert space. Interestingly, the revivals occurred after periods when the evolution was entanglement breaking, indicating a constant transfer of quantum information back and forth between the qubit and bath. Our results were based on a worst-case regime in which the qubit was subjected to an identical transverse field to the bath and in general was found to be less robust against decoherence than the Ising interaction. Thus, systems with Ising interactions coupling only to a small neighborhood of the environment would perform better as quantum memories.

ACKNOWLEDGMENTS

This work was supported by the UK EPSRC through projects QIPIRC (GR/S82176/01) and EuroQUAM (EP/E041612/1).

Appendix A: Quantum Operations Formalism and the Jamiolkowski Isomorphism

A powerful tool for considering the evolution of a quantum system is the quantum operations formalism [1]. If the initial state of the quantum system is described in terms of a density operator ρ, the subsequent evolution causes a transformation to a final state given by the mapping $\rho \rightarrow \varepsilon\{\rho\}$. The linear, completely positive map ε is known as a quantum operation. For a closed system that implements a particular unitary operation U, the quantum operation is simply $\varepsilon(\rho) = U\rho U^{\dagger}$. In the same context, the evolution of an open quantum subsystem interacting with some environment R, e.g. a single spin-1/2 interacting with an LMG spin bath, can be described as

$$\varepsilon(\rho) = \mathrm{Tr}_R[U_T(\rho \otimes \rho_R)U_T^{\dagger}] \ , \tag{A1}$$

where we consider the total system as closed and obtain the final reduced density operator for the principal subsystem by tracing out the state of the environment (note that we assume an initial product state for the subsystem and environment).

Although an elegant description, calculating the final state in the above way is often computationally difficult due to the large size of the total Hilbert space. We can instead express Eq. (A1) explicitly in terms of the principal subsystem's Hilbert space $\mathcal{H}$ by

$$\varepsilon(\rho) = \sum_{i=1}^{d^2} A_i \rho A_i^\dagger \ . \tag{A2}$$

where the A_i, which act on $\mathcal{H}$, are known as Kraus operators and d is the dimension of $\mathcal{H}$. Once the Kraus operators are known for a particular type of evolution, one can easily obtain the final state of the open subsystem given any initial state. Importantly, the Kraus operators reveal the nature of the noise induced by the coupling to the environment. For a unital map, which is always the case for the noise described by the coupling to an environment, the Kraus operators satisfy $\sum_i A_i A_i^\dagger = \mathbb{1}$.

An equivalent description of the evolution in Eq. (A2) can be made in terms of a superoperator Λ. To explain this more fully, consider the Hilbert space $\mathcal{H}$ spanned by basis states $\{|i\rangle \mid i = 0, \cdots, d-1\}$. We can expand any density operator ρ for the system in the operator basis $\{|i\rangle\langle j| \mid i, j = 0, \cdots, d-1\}$, with its corresponding matrix elements ρ_{ij} contained in a d^2-dimensional vector. The superoperator Λ can then be described by a $d^2 \times d^2$ super-matrix with elements

$$\Lambda = \sum_{kl=0}^{d-1} \Lambda_{ij,kl} |k\rangle\langle l| \ . \tag{A3}$$

Note that Λ can be inferred from the Kraus operators and vice versa via

$$\Lambda = \sum_{i=1}^{d^2} A_i^* \otimes A_i \ . \tag{A4}$$

The Jamiolkowski isomorphism [44] exploits an initial setup of two copies of the principal subsystem, such that the subsequent evolution transfers all the information about Λ to the final quantum state. The two copies a and b are prepared in the maximally entangled state $|\Psi^+\rangle = \frac{1}{\sqrt{d}} \sum_{i=0}^{d-1} |i\rangle \otimes |i\rangle$ and the superoperator Λ is applied to b as

$$(\mathbb{1} \otimes \Lambda)\{|\Psi^+\rangle\langle\Psi^+|\} = \frac{1}{d} \sum_{ij=0}^{d-1} |i\rangle\langle j| \otimes \Lambda |i\rangle\langle j| = \rho^\Lambda \ . \tag{A5}$$

The matrix elements of the resulting density operator ρ^Λ are related to those of Λ by $d\rho^\Lambda_{ikjl} = \Lambda_{ijkl}$, where

$$\rho^\Lambda = \sum_{ijkl=0}^{d-1} \rho^\Lambda_{ikjl} |i\rangle\langle j| \otimes |k\rangle\langle l| \ . \tag{A6}$$

Thus, using the Jamiolkowski isomorphism, it is sufficient to calculate ρ^Λ to determine the superoperator Λ, and then trivially the Kraus operators A_i, for any quantum operation $\varepsilon(\rho)$.

Appendix B: The Loschmidt Echo for a single link and an isotropic bath

The GS of an isotropic, ferromagnetically coupled bath is the Dicke state $|N/2, M\rangle$, where $M = N/2$, $\lfloor hN/2\lambda \rfloor$ in the normal and broken phases respectively. For $N \gg 1$ the latter can be approximated as $M = hN/2\lambda$. When we partition the bath into a single and $N-1$ spins the Dicke state $|N/2, M\rangle$ decomposes into two terms

$$\begin{aligned} \left|\tfrac{N}{2}, M\right\rangle = c_{1/2} \left|\tfrac{1}{2}, \tfrac{1}{2}\right\rangle \otimes \left|\tfrac{N}{2} - \tfrac{1}{2}, M - \tfrac{1}{2}\right\rangle \\ + c_{-1/2} \left|\tfrac{1}{2}, -\tfrac{1}{2}\right\rangle \otimes \left|\tfrac{N}{2} - \tfrac{1}{2}, M + \tfrac{1}{2}\right\rangle \ , \end{aligned} \tag{B1}$$

where the Clebsch-Gordon coefficients are given by

$$\begin{aligned} c_{1/2} &= \left\langle \tfrac{1}{2}, \tfrac{1}{2} \right| \otimes \left\langle \tfrac{N}{2} - \tfrac{1}{2}, M - \tfrac{1}{2} \middle| \tfrac{N}{2}, M \right\rangle = \sqrt{\tfrac{1}{2} + \tfrac{M}{N}} \ , \\ c_{-1/2} &= \left\langle \tfrac{1}{2}, -\tfrac{1}{2} \right| \otimes \left\langle \tfrac{N}{2} - \tfrac{1}{2}, M + \tfrac{1}{2} \middle| \tfrac{N}{2}, M \right\rangle = \sqrt{\tfrac{1}{2} - \tfrac{M}{N}} \ . \end{aligned} \tag{B2}$$

Evolution of the GS under the perturbed bath Hamiltonian $H_- = H_R - \epsilon\sigma_1^z$ for this scenario is restricted to the two states on the RHS of Eq. (B1). Using these states as a basis, the action of H_- on the Dicke state $|N/2, M\rangle$ can be summarised by the matrix equation

$$H_- \left|\tfrac{N}{2}, M\right\rangle = h \begin{pmatrix} \alpha - \epsilon/h & \beta \\ \beta & \alpha + \zeta + \epsilon/h \end{pmatrix} \begin{pmatrix} c_{1/2} \\ c_{-1/2} \end{pmatrix} \ , \tag{B3}$$

where

$$\alpha = -\frac{\lambda}{2hN} \left\{ (N-1)^2 - (2M-1)^2 \right\} - 2M \ , \tag{B4}$$

$$\beta = -\frac{\lambda}{h} \sqrt{1 - \frac{4M^2}{N^2}} \ , \tag{B5}$$

$$\zeta = \frac{4\lambda M}{hN} \ . \tag{B6}$$

For $N \gg 1$, the latter two quantities become

$$\beta = -\frac{\lambda}{h} \sqrt{1 - \frac{h^2}{\lambda^2}} \ , \tag{B7}$$

$$\zeta = 2 \ . \tag{B8}$$

By firstly diagonalizing the matrix representation of H_- in Eq. (B3), we can find a similar representation for $e^{-iH_- t}$ in this basis, given by

$$e^{-iH_-t} = \frac{e^{-i(\alpha+1)ht}}{\eta_-}\begin{pmatrix} \eta_-\cos(\eta_-t/2) + 2i(h+\epsilon)\sin(\eta_-t/2) & -2i\beta h\sin(\eta_-t/2) \\ -2i\beta h\sin(\eta_-t/2) & \eta_-\cos(\eta_-t/2) - 2i(h+\epsilon)\sin(\eta_-t/2)\end{pmatrix}, \quad \text{(B9)}$$

where $\eta_- = 2\sqrt{\lambda^2+\epsilon(\epsilon+2h)}$. Similarly, for e^{-iH_+t} we obtain

$$e^{-iH_+t} = \frac{e^{-i(\alpha+1)ht}}{\eta_+}\begin{pmatrix} \eta_+\cos(\eta_+t/2) + 2i(h-\epsilon)\sin(\eta_+t/2) & -2i\beta h\sin(\eta_+t/2) \\ -2i\beta h\sin(\eta_+t/2) & \eta_+\cos(\eta_+t/2) - 2i(h-\epsilon)\sin(\eta_+t/2)\end{pmatrix}, \quad \text{(B10)}$$

where $\eta_+ = 2\sqrt{\lambda^2+\epsilon(\epsilon-2h)}$. The LE for the broken phase ($\lambda > h$) can now be calculated by multiplying the hermitian conjugate of Eq. (B10) by Eq. (B9) and taking the expectation value with respect to the GS, i.e.

$$L(t) = \left| \left(c_{1/2}, c_{-1/2}\right) e^{iH_+t}e^{-iH_-t}\begin{pmatrix} c_{1/2} \\ c_{-1/2}\end{pmatrix}\right|^2. \quad \text{(B11)}$$

The resulting expression for the LE is complicated and need not be written here explicitly. Importantly, we can see revivals of full qubit coherence occur at times $t = l\tau_c$ that satisfy both $\eta_-\tau_c = 2l_-\pi$ and $\eta_+\tau_c = 2l_+\pi$, where l, l_- and l_+ are all integers; at these times the matrices in Eq. (B9) and Eq. (B10) are both equal to the identity. In the limit $\epsilon \ll h$ the two frequencies are approximately equal and the coherence time is $\tau_c = \pi/\lambda$.

[1] M. A. Nielsen and I. L. Chuang, *Quantum Computation and Quantum Information* (Cambridge University Press, 2000).
[2] N. Gisin, G. Ribordy, W. Tittel, and H. Zbinden, Rev. Mod. Phys., **74**, 145 (2002).
[3] H. J. Briegel, W. Dür, J. I. Cirac, and P. Zoller, Phys. Rev. Lett., **81**, 5932 (1998).
[4] L.-M. Duan, M. D. Lukin, J. I. Cirac, and P. Zoller, Nature, **414**, 413 (2001).
[5] A. Acín, J. I. Cirac, and M. Lewenstein, Nat. Phys., **3**, 256 (2007).
[6] S. Broadfoot, U. Dorner, and D. Jaksch, (2009), arxiv:0906.1622.
[7] S. Perseguers, J. I. Cirac, A. Acín, M. Lewenstein, and J. Wehr, Phys. Rev. A, **77**, 022308 (2008).
[8] N. V. Prokof'ev and P. C. E. Stamp, Rep. Prog. Phys., **63**, 669 (2000).
[9] J. M. Taylor, A. Imamoglu, and M. D. Lukin, Phys. Rev. Lett., **91**, 246802 (2003).
[10] J. J. L. Morton, A. M. Tyryshkin, R. M. Brown, S. Shankar, B. W. Lovett, A. Ardavan, T. Schenke, E. E. Haller, J. W. Ager, and S. A. Lyon, Nature, **455**, 1085 (2008).
[11] A. Imamoglu, D. D. Awschalom, G. Burkard, D. P. DiVincenzo, D. Loss, M. Sherwin, and A. Small, Phys. Rev. Lett., **83**, 4204 (1999).
[12] L. Childress, M. V. Gurudev Dutt, J. M. Taylor, A. S. Zibrov, F. Jelezko, J. Wrachtrup, P. R. Hemmer, and M. D. Lukin, Science, **314**, 281 (2006).
[13] W. H. Zurek, Phys. Rev. D, **26**, 1862 (1982).
[14] S. Paganelli, F. de Pasquale, and S. M. Giampaolo, Phys. Rev. A, **66**, 052317 (2002).
[15] H.-P. Breuer, D. Burgarth, and F. Petruccione, Phys. Rev. B, **70**, 045323 (2004).
[16] F. M. Cucchietti, J. P. Paz, and W. H. Zurek, Phys. Rev. A, **72**, 052113 (2005).
[17] H. T. Quan, Z. Song, X. F. Liu, P. Zanardi, and C. P. Sun, Phys. Rev. Lett., **96**, 140604 (2006).
[18] F. M. Cucchietti, S. Fernandez-Vidal, and J. P. Paz, Phys. Rev. A, **75**, 032337 (2007).
[19] Y.-C. Ou and H. Fan, Journ. of Phys. A, **40**, 2455 (2007).
[20] S. Camalet and R. Chitra, Phys. Rev. B, **75**, 094434 (2007).
[21] C.-Y. Lai, J.-T. Hung, C.-Y. Mou, and P. Chen, Phys. Rev. B, **77**, 205419 (2008).
[22] Z.-G. Yuan, P. Zhang, and S.-S. Li, Phys. Rev. A, **75**, 012102 (2007).
[23] L. Tessieri and J. Wilkie, Journ. of Phys. A, **36**, 12305 (2003).
[24] H. T. Quan, Z. D. Wang, and C. P. Sun, Phys. Rev. A, **76**, 012104 (2007).
[25] Y. Hamdouni and F. Petruccione, Phys. Rev. B, **76**, 174306 (2007).
[26] A. Relano, J. M. Arias, J. Dukelsky, J. E. García-Ramos, and P. Pérez-Fernández, Phys. Rev. A, **78**, 060102 (2008).
[27] D. Rossini, T. Calarco, V. Giovannetti, S. Montangero, and R. Fazio, Phys. Rev. A, **75**, 032333 (2007).
[28] J. Vidal, G. Palacios, and R. Mosseri, Phys. Rev. A, **69**, 022107 (2004).
[29] J. Vidal, R. Mosseri, and J. Dukelsky, Phys. Rev. A, **69**, 054101 (2004).
[30] J. I. Latorre, R. Orús, E. Rico, and J. Vidal, Phys. Rev. A, **71**, 064101 (2005).
[31] H. T. Cui, Phys. Rev. A, **77**, 052105 (2008).

[32] R. Orús, S. Dusuel, and J. Vidal, Phys. Rev. Lett., **101**, 025701 (2008).
[33] A. Osterloh, L. Amico, G. Falci, and R. Fazio, Nature, **416**, 608 (2002).
[34] T. J. Osborne and M. A. Nielsen, Phys. Rev. A, **66**, 032110 (2002).
[35] L. Amico, R. Fazio, A. Osterloh, and V. Vedral, Rev. Mod. Phys., **80**, 517 (2008).
[36] G. Vidal, J. I. Latorre, E. Rico, and A. Kitaev, Phys. Rev. Lett., **90**, 227902 (2003).
[37] H. J. Lipkin, N. Meshkov, and A. J. Glick, Nucl. Phys., **62**, 188 (1965).
[38] J. I. Cirac, M. Lewenstein, K. Mølmer, and P. Zoller, Phys. Rev. A, **57**, 1208 (1998).
[39] S. Morrison and A. S. Parkins, Phys. Rev. Lett., **100**, 040403 (2008).
[40] R. H. Dicke, Phys. Rev., **93**, 99 (1954).
[41] R. Botet, R. Jullien, and P. Pfeuty, Phys. Rev. Lett., **49**, 478 (1982).
[42] R. Botet and R. Jullien, Phys. Rev. B, **28**, 3955 (1983).
[43] I. I. Guseinov, A. Ozmen, U. Atav, and H. Yuksel, Journ. Comp. Phys., **122**, 343 (1995).
[44] A. Jamiolkowski, Rep. Math. Phys., **3**, 275 (1972).
[45] P. Zanardi and D. A. Lidar, Phys. Rev. A, **70**, 012315 (2004).
[46] M. Hein, W. Dür, and H.-J. Briegel, Phys. Rev. A, **71**, 032350 (2005).
[47] A. Peres, Phys. Rev. Lett., **77**, 1413 (1996).
[48] M. Horodecki, P. Horodecki, and R. Horodecki, Phys Lett A, **223**, 1 (1996).
[49] A. Peres, *Quantum Theory: Concepts and Methods* (Kluwer Academic, London, 1995).
[50] The scaling with bath size N of the induced phase may make it difficult for one to keep track of this for large baths.
[51] We note that in this scenario the qubit cannot be spectroscopically isolated from the bath ensemble.